

Stability of native defects in hexagonal and cubic boron nitride

Walter Orellana*

Departamento de Física, ICEx, Universidade Federal de Minas Gerais, Caixa Postal 702, 30123-970 Belo Horizonte, Minas Gerais, Brazil

H. Chacham[†]

Department of Physics, University of Texas, Austin, Texas 78712

(Received 17 April 2000; revised manuscript received 24 August 2000; published 12 March 2001)

We investigate, through first-principles calculations, the stability and electronic structure of self-interstitials and vacancies in both hexagonal (graphite-like) and cubic boron nitride. We find that the self-interstitials N_i and B_i in hexagonal boron nitride (h -BN) have low formation energies, comparable to those of the vacancies V_N and V_B . For instance, we find that N_i is the most stable defect in h -BN under N-rich and p -type conditions followed by the nitrogen vacancy. This is consistent with experimental findings of large concentrations of nitrogen interstitials and vacancies, and of the trapping of nitrogen in the hexagonal phase of BN thin films grown by ion-bombardment assisted deposition techniques. In contrast, in cubic boron nitride (c -BN) the self-interstitials have high formation energies as compared to those of the vacancies. As a consequence, the formation of vacancy-interstitial pairs in kickout processes would typically require much more energy in c -BN than in h -BN. This suggests that a possible role of the ion bombardment in favoring the growth of c -BN films is to generate a much larger amount of defects in the hexagonal phase than in the cubic phase.

DOI: 10.1103/PhysRevB.63.125205

PACS number(s): 71.55.Eq, 71.15.Dx, 71.15.Nc

I. INTRODUCTION

Boron nitride (BN) is a compound that occurs in several structures. In a similar way as carbon, BN can occur in sp^2 -bonded structures like hexagonal BN (h -BN), sp^3 -bonded structures like cubic BN (c -BN), as well as nanotube¹ and fullerene^{2,3} structures. The cubic form is one of the hardest materials known to date and for this reason it has attracted considerable attention. The synthesis of bulk cubic BN requires the application of high pressures and temperatures, similar to the synthesis of diamond. However, it has been found in recent years⁴⁻¹⁰ that the growth of cubic boron nitride thin films can be attained by deposition techniques assisted by low-energy ion bombardment (e.g., N_2^+ and Ar^+) during film growth. The formation of the cubic phase is intermediated by an sp^2 -bonded boron nitride layer adjacent to the substrate. The ion bombardment also causes structural damage and compressive stress that can restrict the film thickness up to 100–200 nm,¹¹ representing a serious limitation in the development of c -BN thin films. On the other hand, recent studies by Boyen *et al.*¹² have shown that post-deposition ion bombardment over high quality c -BN thin films leads to a strong relaxation of the compressive stresses without destroying the cubic phase.

Recently, Jiménez *et al.*^{13,14} have applied the near-edge x-ray absorption fine structure spectroscopy (NEXAFS) method to the study of bonding modifications and point defects in BN thin films induced by ion bombardment. These works have identified the presence of nitrogen vacancies and interstitials in h -BN after it is ion bombarded by N_2^+ . They also found B-B bonds formed in the hexagonal-like structure, which have been addressed to boron at interstitial sites or to the formation of boron clusters.

The above experimental results show that the impact of

energetic ions during the growth of BN films has mainly two effects: First, it generates a large amount of defects, notably nitrogen vacancies and interstitials in the hexagonal phase. Second, it favors the growth of the cubic phase relative to the hexagonal phase. The reasons for the abundance of certain defects, and a possible relation between the abundance of defects and the growth of the cubic phase are important and open questions. Consequently, the study and characterization of defects that might be induced in h -BN and c -BN considering typical growth conditions, like electron- or hole-rich environments and stoichiometric variations, are important subjects to be considered from a theoretical point of view.

The purpose of our work is to provide both qualitative and quantitative information on the energetics of formation of native defects and on competing processes involving native defects as induced by ion bombardment in h -BN and c -BN considering the above described growth conditions. We find that the self-interstitials N_i and B_i in h -BN have low formation energies, comparable to those of the vacancies V_N and V_B . For instance, we find that N_i is the most stable defect in h -BN under N-rich and p -type conditions, followed by the nitrogen vacancy. In contrast, the self-interstitials in c -BN have high formation energies as compared to those of the vacancies. As a consequence, the formation of vacancy-interstitial pairs in kickout processes would typically require much more energy in c -BN than in h -BN. In particular, we find that in p -type conditions the formation energy of a distant V_N+N_i pair in h -BN is 3.0 eV, whereas in c -BN the formation energy of the same pair is 8.0 eV. This suggests that a possible role of the ion bombardment in favoring the growth of c -BN films is to generate a much larger amount of defects in the hexagonal phase than in the cubic phase.

Our paper is organized as follows: In Sec. II we describe the first-principles methodology used in the calculations. In

Secs. III A and III B, we discuss our results for the electronic structure and the minimum-energy configuration of the vacancies and self interstitials in *h*-BN and *c*-BN in the several possible charge states. In Sec. III C, we perform a comparative study on the energetics of the formation of vacancies, self-interstitials, and vacancy-interstitial distant pairs in *h*-BN and *c*-BN as a function of the electron-chemical potential. Finally, In Sec. IV we present a summary of our results.

II. THEORETICAL METHOD

Our calculations are performed in the framework of the density-functional theory,¹⁵ the first-principles pseudopotential method, and a plane-wave basis set. For the exchange-correlation potential we use the generalized-gradient approximation (GGA).¹⁶ Boron and nitrogen pseudopotentials are generated by the scheme of Troullier and Martins.¹⁷ We use a plane-wave energy cutoff of 60 Ry. All the atoms in the graphitelike and zinc-blende structures are fully relaxed according to the calculated Hellmann-Feynman forces on ions until these forces are negligible (less than 0.05 eV/Å), assuming no symmetry constraints.

The hexagonal BN structure has D_{6h} symmetry with four atoms per unit cell. It exhibits an *AB*-like stacking sequence with each boron atom on top of a nitrogen atom. We use a 64-atom supercell consisting of $4 \times 4 \times 2$ the unit cell. We calculate the equilibrium structure by minimizing the total energy with respect to the *a* and *c* parameters. Our results for the equilibrium lattice constants are $a = 2.483$ Å and $c = 6.701$ Å, which are within 1% of the experimental values ($a = 2.504$ Å and $c = 6.66$ Å).¹⁸

For the Brillouin-zone sampling we use a single **k** point (the Γ point). To check the convergence of the total energy and the atomic geometry for the one **k**-point sampling, we perform a vacancy calculation by considering three **k** points. Our results show that the variations in the total energy with respect to the one **k**-point calculation are less than 0.03 eV/atom with negligible differences in the atomic geometry. Our results for the electronic structure show a direct gap at the Γ point of 4.9 eV and an indirect gap ($K \rightarrow M$) of 4.0 eV. These results are in close agreement with recent total-energy calculations.¹⁹

For cubic BN we use a supercell of 64 atomic sites in the zinc-blende structure. We find the equilibrium lattice constant $a = 3.617$ Å and the bulk modulus $B = 3.69$ Mbar, which are in good agreement with the experimental values ($a = 3.615$ Å and $B = 3.80$ Mbar).²⁰ The electronic structure shows an indirect gap ($\Gamma \rightarrow X$) of 4.8 eV. For the Brillouin zone sampling we also use the Γ point. Checks of convergence with four **k** points show that variations in the total energies are less than 0.04 eV/atom.

The formation energies of vacancies and interstitials in *h*-BN and *c*-BN are calculated as a function of the chemical potentials of both atomic species, μ_B and μ_N , and the electron chemical potential or Fermi level μ_e .²¹ For instance, in the case of the N interstitial in the charge state *q*, the formation energy is given by

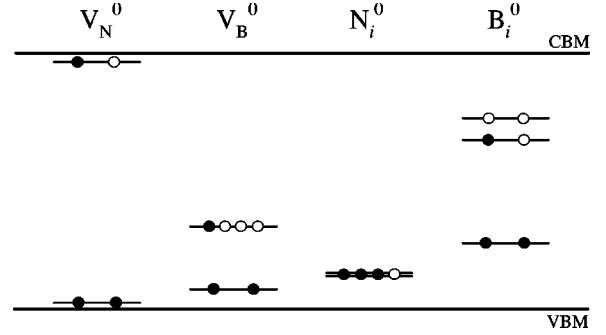


FIG. 1. Schematic representation of the single-particle energy levels induced by neutral vacancies and self-interstitials in *h*-BN in the band gap. The filled dots indicate electrons and the open dots indicate holes.

$$E_f(N_i^q) = E_i(N_i^q) - n_N \mu_N - n_B \mu_B + q(\mu_e + \epsilon_v), \quad (1)$$

where E_i is the total energy and n_N (n_B) is the number of N (B) atoms in the supercell. The Fermi level μ_e is measured with respect to the energy of the valence-band maximum ϵ_v . The chemical potentials of the B and N atoms vary over a range given by the heat of formation of the respective BN bulk structure, defined as $H_f(\text{BN}) = E_{\text{BN}} - E_{\text{B}(\text{bulk})} - E_{\text{N}(\text{bulk})}$. We calculate $H_f(\text{c-BN}) = -3.0$ eV and $H_f(\text{h-BN}) = -3.3$ eV. Additionally, the atomic chemical potentials are constrained by the thermal equilibrium condition $\mu_B + \mu_N = \mu_{\text{BN}}$. The upper bound for μ_N is assumed to be the precipitation limit on its bulk phase, $\mu_N \leq \mu_{\text{N}(\text{bulk})}$. Fixing μ_N to its maximum value in Eq. (1) results in a N-rich condition for the formation energies. For the $\mu_{\text{N}(\text{bulk})}$ calculation we have considered the nitrogen ground-state structure α -N₂. Details of those bulk structure calculations can be found in Ref. 22.

Recent calculations by Kern *et al.*²³ indicate that the local density approximation (LDA) predicts larger cohesive energies than those calculated within the GGA approach for systems bound by weak intermolecular forces, like *h*-BN planes. In addition, they found that GGA calculations would fail in predicting the stability of the *h*-BN structure. Although a similar trend between LDA and GGA has been detected in the present work, we find that both approximations for the exchange-correlation functional, result in positive cohesive energies for the interaction between BN planes in *h*-BN (0.03 eV for GGA and 0.09 eV for LDA). In the present work, we have chosen to use the GGA approach because it better predicts cohesive energies of solids (see, for instance, Ref. 23), which is a quantity closely related to defect-formation energies.

III. RESULTS AND DISCUSSION

A. Defects in *h*-BN: Geometry and electronic structure

Figure 1 shows a schematic representation of the single-particle energy levels induced by neutral vacancies (V_N^0 ,

V_B^0) and self-interstitials (N_i^0 , B_i^0) in h -BN inside the theoretical band gap (4.0 eV). According to our GGA calculation, V_B^0 induces a fully occupied singlet (nondegenerated) level at $\epsilon_v + 0.31$ eV and a singly occupied doublet (degenerated) level at $\epsilon_v + 1.29$ eV, where ϵ_v is the valence-band maximum. Therefore, the neutral boron vacancy in h -BN behaves as a triple acceptor. For V_N^0 we find two singlet levels close to the edges of the band gap, at $\epsilon_v + 0.10$ eV and $\epsilon_v + 3.86$ eV. The uppermost singlet level is half occupied suggesting that the neutral nitrogen vacancy in h -BN behaves as a single donor.

Regarding the equilibrium geometry, the three first-neighbor B atoms of V_N^0 undergo a small outward relaxation of 0.02 Å ($\sim 1\%$) with respect to the unrelaxed positions. Whereas for V_B^0 , their first-neighbor N atoms show a larger outward relaxation of 0.1 Å ($\sim 7\%$). Similar relaxations are also observed in other charge states of the vacancies (1+ to 3+ for V_N and 1+ to 3- for V_B).

In order to find the minimum-energy configuration of self-interstitials in h -BN we have considered different interstitial sites for the N and B impurities in the graphitelike structure before starting the molecular-dynamics calculation. We choose two on-layer sites, at the center of the hexagon and between a B-N bond, and two interlayer sites, at the center of the hexagon and between B and N atoms.

Figure 2(a) shows the total electronic-charge density of N_i^0 in its lower-energy configuration. We observe that the interstitial nitrogen binds strongly with a N atom of the lattice forming a N-N pair with bond distance of 1.55 Å, which is approximately 30% larger than that of the N_2 molecule (1.1 Å). This pair is oriented normal to the layer binding equally with their three first-neighbor B atoms with a B-N bond distance of 1.61 Å. This configuration is also found in other charge states of the defect. The electronic structure of N_i^0 shows two nearly degenerate singlet levels in the band gap at $\epsilon_v + 0.54$ eV and $\epsilon_v + 0.55$ eV, occupied with two and one electron respectively (see Fig. 1). Figure 2(b) shows the electronic charge density associated to the singly-occupied gap level. We observe a π -like character at the N-N pair and more localized p_z -like character at the neighboring N atoms of the same layer. The above results suggest that this level can be described as a perturbation of the highest occupied molecular orbital state of the perfect h -BN lattice, which is composed by p_z -like dangling bonds located at the nitrogen atoms of the lattice.¹⁹

Our results for the lower-energy configuration of B_i^0 show the interstitial B atom in an interlayer position bonding with both N and B atoms of adjacent planes, as shown in Fig. 3(a). We also find that in 1+ and 2+ charge states, the B impurity is almost in line with the N and B atoms of the adjacent layers. However, for neutral, 1- and 2- charge states the B impurity binds with a B atom of the first layer and with a B-N pair of the second layer tending to form B-B-B bonds with the addition of extra electrons. In these charge states, both layers undergo large distortions in the neighborhood of the interstitial. On the other hand, for the 3- charge state we observe that the interstitial B atom moves closer to the N atom tending to form a B-N pair occupying the N site in the layer but preserving the bond

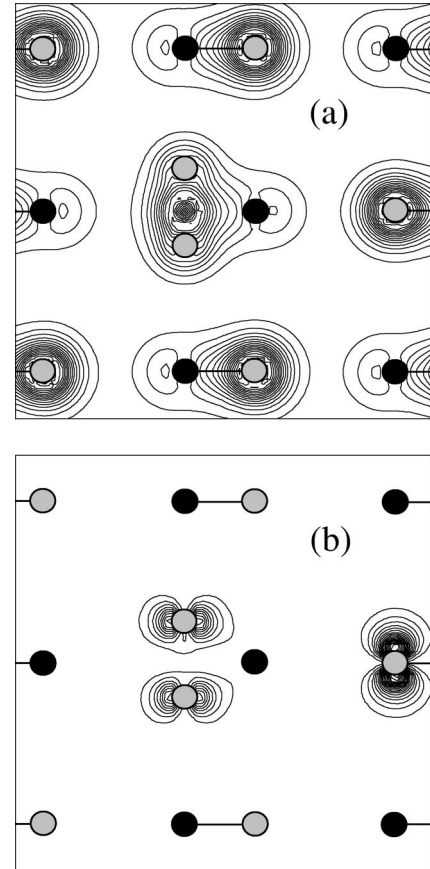


FIG. 2. Wave-function squared plots of interstitial nitrogen in h -BN in the lowest-energy configuration. (a) For all occupied single-particle energy levels. (b) For half-occupied gap level. The plane is displayed perpendicular to the h -BN layers passing through B-N bonds. Black circles represent B atoms and gray circles represent N atoms.

with the B atom of the adjacent layer. In this geometry, the interstitial B atom binds with four neighboring B atoms. The above results are in good agreement with experimental observations of B-B bond sequences and the tendency of B atoms to form small clusters in h -BN.¹⁴ In addition, our results suggest that the formation of B clusters would be more likely to occur for n -type growth conditions.

The electronic structure of B_i^0 (see Fig. 1) shows three singlet levels in the band gap: A fully occupied one at $\epsilon_v + 1.03$ eV, a half-occupied one at $\epsilon_v + 2.64$ eV, and an empty level at $\epsilon_v + 2.98$ eV. These energy levels are related to the metalliclike B-B bonds as shown in the charge-density plot for the half-occupied gap level in Fig. 3(b).

We also calculate the total energy of both N and B interstitials fixed at nonbonded positions in the h -BN lattice. This was done in order to estimate the gain in energy of the minimum-energy configurations with respect to nonbonded positions. The energy difference between both configurations can be interpreted as the binding energy of the interstitial atoms. For the nonbonded interstitial site we choose an interlayer position in the center of a hexagon. Our results show a gain in energy of 1.5 eV for B_i and of 2.9 eV for N_i . The large difference in energy between the nonbonded interstitial

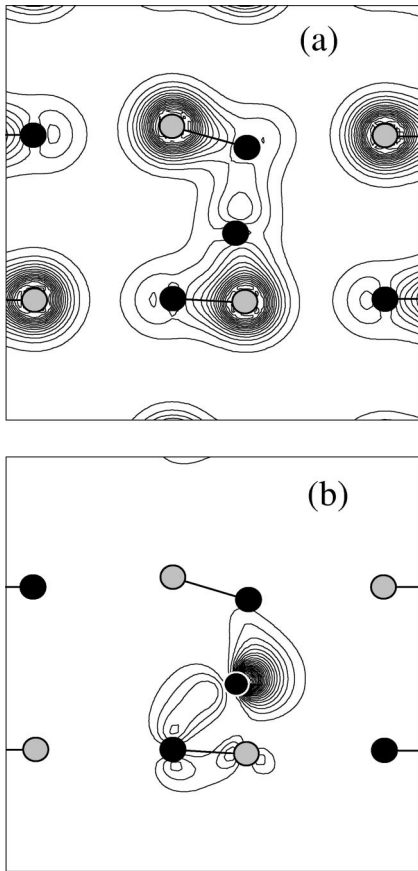


FIG. 3. Wave-function squared plots of interstitial boron in *h*-BN in the lowest-energy configuration. (a) For all occupied single-particle energy levels. (b) For the half-occupied gap level. The plane is displayed perpendicular to the *h*-BN layers passing through B-N bonds. Black circles represent B atoms and gray circles represent N atoms.

position and the final equilibrium position indicate that the bonds of the B_i and N_i defects are very strong, especially for the N-N pair that has almost twice the binding energy of the B-B-B bonded structure.

B. Defects in *c*-BN: Geometry and electronic structure

Figure 4 shows schematically the single-particle energy levels induced by neutral vacancies and self-interstitials in *c*-BN inside the theoretical band gap (4.8 eV). In a previous work,²² we have discussed in more detail the electronic and structural properties of the boron and nitrogen vacancies in *c*-BN within the same theoretical approach as presented in this work. In the following, we discuss the electronic structure and equilibrium geometry of B and N interstitials in *c*-BN.

In the same way as performed in the graphitelike structure, we calculate the minimum-energy atomic geometry of self-interstitials in *c*-BN by considering different interstitial sites in the zinc-blende structure before starting the molecular-dynamics calculation. These sites are: Between a B-N bond (bonding site), the sites opposite to the bonding

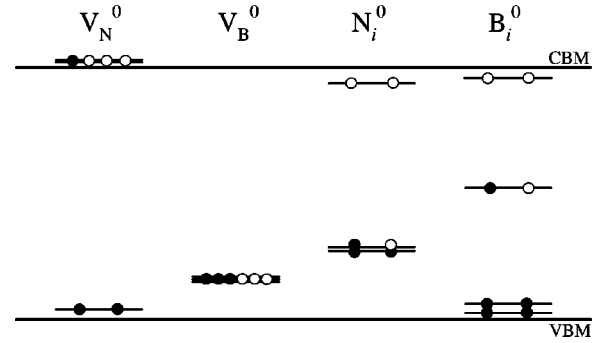


FIG. 4. Schematic representation of the single-particle energy levels induced by neutral vacancies and self-interstitials in *c*-BN in the band gap. The filled dots indicate electrons and the open dots indicate holes.

site with respect to the B and N atoms, and the tetrahedral sites surrounded by B and N atoms.

Our results for the minimum-energy configuration of N_i^0 show the formation of a N-N pair occupying a nitrogen site of the lattice, as also observed in the *h*-BN structure. In this split-interstitial configuration, each N atom of the pair binds with two first-neighbor B atoms. The N-N bond distance for the neutral defect is found to be of 1.28 Å, which is 16% larger than that of the N_2 molecule. We find equal bond distances between a nitrogen atom of the pair and the neighboring B atoms of 1.42 Å, with a B-N-B angle of 141°. This configuration is also found in others charge states of the defect.

The electronic structure of N_i^0 (see Fig. 4) shows three singlet levels in the band gap: A fully occupied one at $\epsilon_v + 1.31$ eV, a half-occupied one at $\epsilon_v + 1.38$ eV, and an empty level close to the bottom of the conduction band at $\epsilon_v + 4.5$ eV. Both midgap levels are associated with two lone pairs located at each N atom of the N-N pair, which are oriented normal to the plane formed by the B-N-B atoms.

The equilibrium geometry of B_i^0 shows a N-B pair occupying a nitrogen site of the lattice also forming a split-interstitial configuration. The bond distance of the N-B pair is found to be 1.32 Å, which is 15% shorter than the bond distance of N-B in bulk *c*-BN. The nitrogen of the pair binds with two first-neighbor B atoms, with a bond distance of 1.42 Å and a B-N-B angle of 140°. Similarly, the boron atom of the pair binds with the two remaining first-neighbor B atoms, with bond distances of 1.52 Å and B-B-B angle of 141°. The above configuration for B_i is found stable for all the charge states investigated.

The electronic structure of B_i^0 (see Fig. 4) shows four singlet levels in the band gap: Two fully occupied levels close to the top of the valence band at $\epsilon_v + 0.13$ and $\epsilon_v + 0.30$ eV, a half-occupied level at $\epsilon_v + 2.51$ eV, and an empty level close to the bottom of the conduction band at $\epsilon_v + 4.60$ eV. Similarly to N_i , the half-occupied level of B_i is associated with a single lone pair located at the N atom of the N-B pair, which is oriented normal to the plane formed by the B-N-B atoms.

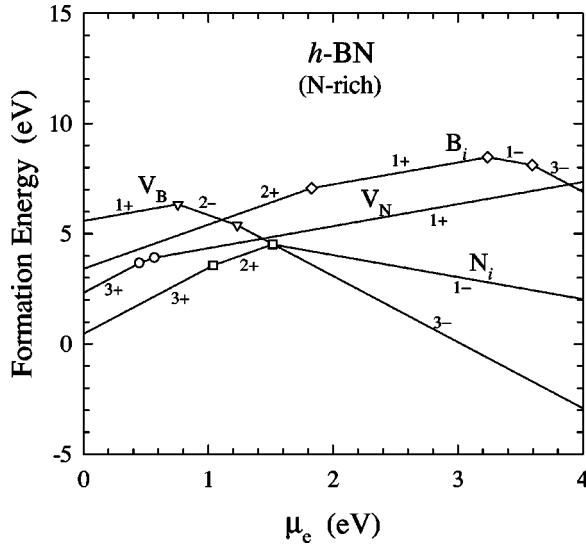


FIG. 5. Formation energies as a function of the Fermi level μ_e for vacancies and interstitials in h -BN for a nitrogen-rich growth condition. The symbols indicate ionization levels and the numbers on the lines indicate defect charge states.

C. Energetics of the native defects: h -BN versus c -BN

The formation energies of V_N , V_B , N_i , and B_i defects in h -BN have been calculated according to Eq. (1) for the range of electron-chemical potentials μ_e between the valence-band maximum and the conduction-band minimum. For a given value of μ_e , the energetically stable charge state q of a given defect is the one that gives the lowest formation energy. The final result is shown in Fig. 5, where the formation energies of the native defects in h -BN under N-rich conditions are plotted as a function of μ_e . The symbols at the cusps of each curve correspond to the values of μ_e where two charge states coexist. These values of μ_e are the ionization levels of the defects. Between consecutive ionization levels, the charge state of the defects are indicated in the figure. The formation energies of the same defects in c -BN under N-rich conditions are shown in Fig. 6.

Figure 5 shows that N_i^{3+} is the most stable defect in h -BN for p -type conditions (small values of μ_e), followed closely by V_N^{3+} and B_i^{2+} . On the other hand, for n -type conditions (large values of μ_e), the most stable defects are V_B^{3-} and N_i^{1-} . Therefore, according to our formation-energy results we conclude that the interstitial N atom can be easily incorporated in h -BN under N-rich growth conditions forming a strong N-N molecular bond. This structure is specially favorable for p -type materials where it exhibits the lower formation energies among the native defects under study. On the other hand, boron vacancies are more likely to occur in n -type materials.

Figure 6 shows that the vacancies are the most stable defects in c -BN while the interstitials have higher formation energies. Therefore, N and B interstitials in c -BN would be unlikely to occur in significant concentrations. This contrasts with Fig. 5, which shows that interstitials in h -BN have formation energies comparable to or lower than those of vacan-

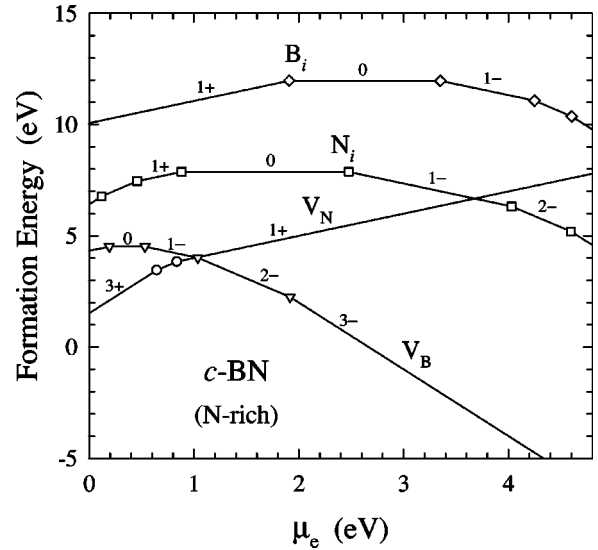


FIG. 6. Formation energies as a function of the Fermi level μ_e for vacancies and interstitials in c -BN for a nitrogen-rich growth condition. The symbols indicate ionization levels and the numbers on the lines indicate defect charge states.

cies. Supposing that the bombardment with positive ions (N_2^+) induces a p -type condition for the resulting material, our results suggest that N_i and V_N in h -BN, and V_N in c -BN are energetically favorable defects in these materials after they are ion-bombarded. In the same condition (p -type), the boron vacancy in h -BN would have a high formation energy. This is consistent with the NEXAFS experiments of Refs. 13 and 14 that indicate the presence of nitrogen vacancies and interstitials in h -BN but do not find evidence of boron vacancies in h -BN and c -BN after N_2^+ bombardment.

In the experimental work of Jiménez *et al.*,¹⁴ a feature in the $N(1s)$ edge of photoabsorption spectra of several BN thin films is clearly associated with the c -BN phase in the samples. The authors of Ref. 14 suggest that this feature is related to nitrogen interstitials in the c -BN phase. Our results show (see Fig. 6) that the formation of nitrogen interstitials in c -BN requires a large amount of energy. Therefore, according to our results this defect should not occur in large concentrations and, consequently, it should not be expected in photoabsorption measurements. We suggest, instead, that the c -BN related feature in the photoabsorption experiments is associated with the nitrogen antisite N_B in c -BN, which has a small formation energy in N-rich conditions²² and could induce an additional feature in the $N(1s)$ edge.

In Fig. 5 we also note that in h -BN the defects V_B^0 , V_B^{1-} , N_i^0 , N_i^{1+} , B_i^0 , and B_i^{2-} are unstable against other charge states of the same defects suggesting that they would exhibit sizable negative- U terms. The largest U energy is found for the $(1-/1+)$ transition state of the B_i defect being approximately of -1.5 eV, whereas this behavior is not observed in c -BN. We believe that the distinct behavior in h -BN is due to the strong lattice relaxation exhibited by V_B , N_i , and B_i when they capture an electron from a singly-occupied gap level or lose an electron from a fully occupied gap level. These lattice relaxations are stronger in h -BN than in c -BN.

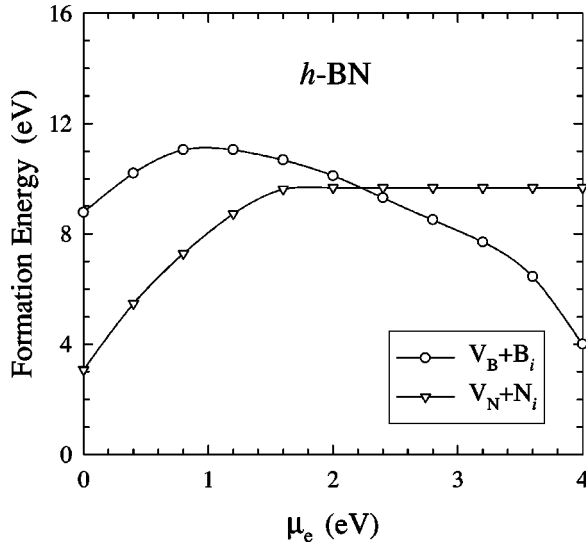


FIG. 7. Formation energies as a function of the Fermi level μ_e for the noninteracting vacancy-interstitial pairs in h -BN.

This might be attributed to the hardness of h -BN crystal that is significantly lower than that of c -BN.

Another characteristic of the energetics of the native defects in h -BN under N-rich conditions, shown in Fig. 5, is that the formation energy of the nitrogen interstitial is smaller than the formation energy of the nitrogen vacancy for any value of the electron chemical potential. This indicates that nitrogen vacancies would provide an efficient trap for nitrogen molecules in the formation of nitrogen interstitials in h -BN. This is consistent with the experimental observation of the trapping of nitrogen in V_N -rich h -BN films bombarded by N_2^+ ions.¹⁴

The above results for the formation energies of the isolated defects are relevant to defect formation during growth processes near thermodynamical equilibrium. However, some growth techniques involve processes that place the growing material far from thermodynamical equilibrium. This is possibly the case of the growth of BN films assisted by N_2^+ implantation.^{13,14} This process results in the growth of films with either sp^3 or sp^2 bonding, depending on growth conditions. Without the ion implantation, only sp^2 bonding occurs. In BN films grown by ion implantation, a large quantity of nitrogen vacancies is also observed as well as nitrogen interstitials.^{13,14}

To investigate the energetics of defect formation due to ion implantation, a possible approach is to consider vacancy-interstitial pairs generated by kickout collisions with the incoming ions. We will consider the energetics of the formation of V_N+N_i and V_B+B_i noninteracting pairs in both h -BN and c -BN. The results of the formation energies of such pairs are shown in Figs. 7 and 8 as a function of the electron-chemical potential μ_e .

Figures 7 and 8 show a striking difference between the energetics of the formation of vacancy-interstitial long-distance pairs in h -BN and the corresponding energetics in c -BN. The curves for h -BN are shifted to lower values, rela-

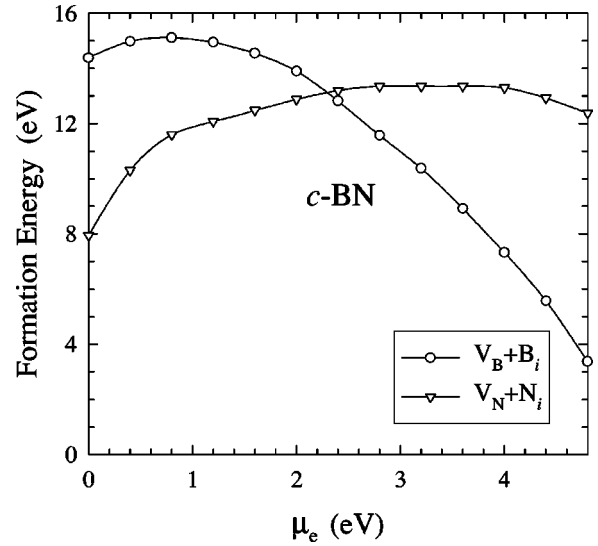


FIG. 8. Formation energies as a function of the Fermi level μ_e for the noninteracting vacancy-interstitial pairs in c -BN.

tive to those of c -BN, by about 5 eV. Such a large difference indicates that, from an energetic point of view, it is much likely that vacancy-interstitial pairs are produced by kickout processes in h -BN than in c -BN.

Although the description of the kinetics of growth of BN films is beyond the scope of the present work, the large energy difference mentioned above suggests that a possible role of the ion bombardment in favoring the growth of c -BN films is to generate a much larger amount of defects in the hexagonal phase than in the cubic phase.

IV. SUMMARY

We have investigated the electronic and structural properties as well as the energetics of isolated vacancies and self-interstitials in h -BN and c -BN using pseudopotential total-energy calculations. Our results show that the boron and nitrogen interstitials and the nitrogen vacancy in p -type, N-rich h -BN have low formation energies suggesting that they are likely to occur under these conditions. This is consistent with the experimental observation of large concentrations of nitrogen interstitials and vacancies, and of the trapping of nitrogen in the hexagonal phase of BN thin films grown by ion-bombardment-assisted deposition techniques. Special attention is given to both interstitials that can transform the bonding structure in their neighborhood inducing important distortions in the h -BN lattice. The interstitial B atom is found at an interlayer position forming metalliclike bonds with B atoms of adjacent layers. On the other hand, the interstitial N atom forms a strong N-N molecular bond with a N atom of the lattice occupying its site. This N-N pair binds equally with its three neighboring B atoms.

The energetics of vacancy-interstitial distant pairs in h -BN indicates that V_N and N_i are energetically favorable defects to be created by kickout processes in p -type materials. In c -BN the formation energy of the same pair, under the same growth conditions, is ~ 5 eV higher in energy than in

the *h*-BN structure. Such a large energy difference suggests that a possible role of the ion bombardment in favoring the growth of *c*-BN films is to generate a large amount of defects in the hexagonal phase but not in the cubic phase.

ACKNOWLEDGMENTS

This work was supported by the Brazilian agencies CNPq, CAPES, and FAPEMIG. The calculations were performed at CENAPAD-MG/CO and LNCC-RJ.

-
- *Present address: Instituto de Física, Universidade de São Paulo, CP 66318, 05315-970, São Paulo, SP, Brazil.
- †Permanent address: Departamento de Física, ICEX, Universidade Federal de Minas Gerais, CP 702, 30123-970, Belo Horizonte, MG, Brazil.
- ¹N.G. Chopra, R.J. Luyken, K. Cherrey, V.H. Crespi, M.L. Cohen, S.G. Louie, and A. Zettl, *Science* **26**, 966 (1995).
- ²D. Goldberg, Y. Bando, O. Stephan, and K. Kurashima, *Appl. Phys. Lett.* **73**, 2441 (1998).
- ³S.S. Alexandre, M.S.C. Mazzoni, and H. Chacham, *Appl. Phys. Lett.* **75**, 61 (1999).
- ⁴D.J. Kestler, K.S. Ailey, R.F. Davis, and K.L. More, *J. Mater. Res.* **8**, 1213 (1993).
- ⁵D.L. Medlin, T.A. Friedmann, P.B. Mirkarimi, P. Rez, M.J. Mills, and K.F. McCarty, *J. Appl. Phys.* **76**, 295 (1994).
- ⁶H. Luethje, K. Bewilogua, S. Daoud, M. Johansson, and L. Hultman, *Thin Solid Films* **257**, 40 (1995).
- ⁷S. Watanabe, S. Miyake, W. Zhou, Y. Ikuhara, T. Suzuki, and M. Murakawa, *Appl. Phys. Lett.* **66**, 1478 (1995).
- ⁸H. Hofsaess, C. Ronning, U. Griesmeier, M. Gross, S. Reinke, M. Kuhr, J. Zweck, and R. Fischer, *Nucl. Instrum. Methods Phys. Res. B* **106**, 153 (1995).
- ⁹T. Ichiki, S. Amagi, and T. Yoshida, *Appl. Phys. Lett.* **79**, 4381 (1996).
- ¹⁰Y. Yamada, O. Tsuda, Y. Tatebayashi, and T. Yoshida, *Thin Solid Films* **295**, 137 (1997).
- ¹¹D.R. McKenzie, W.D. McFall, W.G. Sainty, C.A. Davis, and R.E. Collins, *Diamond Relat. Mater.* **2**, 970 (1993).
- ¹²H.-H. Boyen, P. Widmayer, D. Schwertberger, N. Deyneka, and P. Ziemann, *Appl. Phys. Lett.* **76**, 709 (2000).
- ¹³I. Jiménez, A. Jankowski, L.J. Terminello, J.A. Carlisle, D.G.J. Sutherland, G.L. Doll, J.V. Mantese, W.M. Tong, D.K. Shuh, and F.J. Himpsel, *Appl. Phys. Lett.* **68**, 2816 (1996).
- ¹⁴I. Jiménez, A. Jankowski, L.J. Terminello, D.G.J. Sutherland, J.A. Carlisle, G.L. Doll, W.M. Tong, D.K. Shuh, and F.J. Himpsel, *Phys. Rev. B* **55**, 12 025 (1997).
- ¹⁵P. Hohenberg and W. Kohn, *Phys. Rev.* **136**, B864 (1964); W. Kohn and L.J. Sham, *Phys. Rev.* **140**, A1133 (1965).
- ¹⁶J.P. Perdew, J.A. Chevary, S.H. Vosko, K.A. Jackson, M.R. Pederson, D.J. Singh, and C. Fiolhais, *Phys. Rev. B* **46**, 6671 (1992).
- ¹⁷N. Troullier and J.L. Martins, *Phys. Rev. B* **43**, 1993 (1991).
- ¹⁸R.W.G. Wyckoff, *Crystal Structure* (Interscience, New York, 1965), Vol. 1.
- ¹⁹X. Blase, A. Rubio, S.G. Louie, and M. Cohen, *Phys. Rev. B* **51**, 6868 (1995).
- ²⁰E. Knittel, R.M. Wentzcovitch, R. Jeanloz, and M. Cohen, *Nature (London)* **337**, 349 (1989).
- ²¹J.E. Northrup and S.B. Zhang, *Phys. Rev. B* **7**, 6791 (1993).
- ²²W. Orellana and H. Chacham, *Appl. Phys. Lett.* **74**, 2984 (1999).
- ²³G. Kern, G. Kresse, and J. Hafner, *Phys. Rev. B* **59**, 8551 (1999).